ARTICLE

Histone deacetylase inhibitor givinostat attenuates nonalcoholic steatohepatitis and liver fibrosis

He-ming Huang[1,2], Shi-jie Fan[2,3], Xiao-ru Zhou[2], Yan-jun Liu[1,2], Xiao Li[2,3], Li-ping Liao[2,3], Jing Huang[2,3], Cui-cui Shi[1], Liang Yu[2], Rong Fu[1,2], Jian-gao Fan[1], Yuan-yuan Zhang[2], Cheng Luo[2,3] and Guang-ming Li[1]

Nonalcoholic steatohepatitis (NASH) is a common chronic liver disease that is increasingly prevalent worldwide. Liver inflammation is an important contributor to disease progression from nonalcoholic fatty liver (NAFL) to NASH, but there is a lack of efficient therapies. In the current study we evaluated the therapeutic potential of givinostat, a histone deacetylase (HDAC) inhibitor, in the treatment of NASH in vivo and in vitro. Liver inflammation was induced in mice by feeding a methionine- and choline-deficient diet (MCD) or a fructose, palmitate, cholesterol diet (FPC). The mice were treated with givoinostat (10 mg·kg^{-1}·d^{-1}, ip) for 8 or 10 weeks. At the end of the experiment, the livers were harvested for analysis. We showed that givoinostat administration significantly alleviated inflammation and attenuated hepatic fibrosis in MCD-induced NASH mice. RNA-seq analysis of liver tissues form MCD-fed mice revealed that givinostat potently blocked expression of inflammation-related genes and regulated a broad set of lipid metabolism-related genes. In human hepatocellular carcinoma cell line HepG2 and human derived fetal hepatocyte cell line L02, givinostat significantly decreased palmitic acid-induced intracellular lipid accumulation. The benefit of givinostat was further confirmed in FPC-induced NASH mice. Givinostat administration significantly attenuated hepatic steatosis, inflammation as well as liver injury in this mouse model. In conclusion, givinostat is efficacious in reversing diet-induced NASH, and may serve as a therapeutic agent for the treatment of human NASH.

Keywords: nonalcoholic steatohepatitis; inflammation; histone deacetylase inhibitor; givinostat; epigenetics

INTRODUCTION

Nonalcoholic fatty liver disease (NAFLD), a complicated liver metabolic disease, has become the most common chronic liver disease [1] and is considered as one of the leading causes of end-stage liver disease. The spectrum of NAFLD ranges from simple liver steatosis to nonalcoholic steatohepatitis (NASH). In western countries approximately one third population is potentially affected by NAFLD, which is related to obesity and type 2 diabetes mellitus [2]. During the past few years, a growing number of people are suffering from NAFLD and the disease is increasingly prevalent worldwide. Modeling studies demonstrate that the prevalence of NAFLD will continue to rise in the next decade [3, 4]. Progressive form of NAFLD, NASH, which is accompanied by liver injury and inflammation can progress to liver fibrosis, cirrhosis, and even hepatocellular carcinoma (HCC) [5]. NASH has increasingly become an enormous clinical and economic burden, and cirrhosis and HCC caused by NASH will soon become a primary indication for liver transplantation [6], yet there is still a lack of efficient pharmacological therapies for the treatment of NASH.

Hepatic inflammatory response is a crucial driving force of disease progression, fueling the transition from NAFL to NASH [7–9]. Inflammation is not only central to the disruption of metabolic homeostasis in the liver but promotes sustained hepatic fibrogenesis and is present in virtually all patients with hepatic fibrosis. It was also reported that patients' inflammation level correlates with hepatic fibrosis progression [10, 11]. Macrophages, including liver resident macrophages (Kupffer cells) and recruited monocyte-derived macrophages, are key players of hepatic inflammation. In NASH, free fatty acids (FFA) stimulate the production of a series of proinflammatory mediators including IL-1β, IL-6, CCL5 in hepatocyte and commit macrophage toward an inflammatory activated state. The activation of macrophage further leads to hepatic stellate cell (HSC) activation and extracellular matrix (ECM) secretion and deposition. Macrophages can produce and activate the archetypal pro-fibrotic cytokine TGF-β and other soluble mediators which can act on the HSCs to induce a pro-fibrotic phenotype [12]. Macrophage-HSC crosstalk is also mediated by IL-1 and TNFα, neutralization of which lead to decreased fibrosis in mouse models [13, 14]. Previous animal studies and early clinical trials showed promising results specifically targeting macrophages. Depletion of macrophages by clodronate liposome or gadolinium chloride in high fat diet-fed mice delayed the development of steatosis, and decreased expression of inflammatory cytokines and fibrosis-related genes [15, 16]. Pharmacological polarization of macrophages

[1]Department of Gastroenterology, Xinhua Hospital, School of Medicine, Shanghai Jiaotong University, Shanghai 200092, China; [2]Drug Discovery and Design Center, State Key Laboratory of Drug Research, Shanghai Institute of Materia Medica, Chinese Academy of Sciences, Shanghai 201203, China and [3]University of Chinese Academy of Sciences, Beijing 100049, China
Correspondence: Yuan-yuan Zhang (zhangyy@simm.ac.cn) or Cheng Luo (cluo@simm.ac.cn) or Guang-ming Li (liguangming@xinhuamed.com.cn)
These authors contributed equally: He-ming Huang, Shi-jie Fan, Xiao-ru Zhou

Givinostat attenuates NASH and liver fibrosis
HM Huang et al.

942

towards anti-inflammatory M2 phenotype partially reversed steatosis. Inhibition of CCL2/CCR2 or CCL5/CCR5, which targets monocyte recruitment, has been shown to attenuate liver fibrosis [7, 17–19], and the CCR2/5 antagonist cenicriviroc is now in a phase 2 clinical trial [20]. Therefore, targeting inflammation may help alleviate hepatic steatohepatitis and fibrosis and prevent the progression of NASH, thus representing a therapeutic strategy for treatment of NASH [21].

Epigenetics, an inheritable phenomenon that affects gene expression without altering the DNA sequence, provided a new perspective on the pathogenesis of NAFLD/NASH [22]. Epigenetic alterations occurred during the adaption of hepatocytes to the lipotoxic environment, inflammation and oxidative stress, orchestrating the reprogramming of transcriptional machinery, and contributing to the pathology of NASH [23]. DNA methylation has not only been suggested to be involved in the progression of NAFLD towards advanced fibrotic clinical stages but also could affect NAFLD-related metabolic phenotypes, such as insulin resistance. Moreover, some epigenetic enzymes are starting to spring up in the biological background of NAFLD. For example, the histone methyltransferase Suv39h2 has been reported to contribute to NASH pathogenesis by promoting the inflammatory response in hepatocytes and macrophages. Suv39h2 deficiency in knockout mice protects the mice from NASH, thus Suv39h2 is considered as a potential target for the development of novel therapeutic solutions [24]. Epigenetic machinery, has been shown to be highly involved in the regulation of inflammatory response [25, 26], yet its role in pathogenesis of NASH and whether drugs targeting epigenetic enzymes could be used for NASH treatment remains poorly studied. Given the crucial role of epigenetic machinery in regulation of inflammation, which is associated with NASH progression, epigenetic inhibitors might show great potential in exploring and discovering novel therapies for treatment of NASH.

In this study, we analyzed previous experimental data [27], and identified the HDAC inhibitor (HDACi) givinostat as the most potent hit, which inhibited macrophages activation in vitro. In a methionine- and choline-deficient diet (MCD) mouse model, givinostat significantly alleviated hepatic inflammation and liver fibrosis. And in hepatocyte and fructose, palmitate, cholesterol diet (FPC) mouse model it was verified that givinostat could not only remit inflammation but also diminish intracellular lipid accumulation, making it a promising drug candidate for developing new therapy for treatment of NASH.

MATERIALS AND METHODS
Animals experiments
Male C57BL/6J 8- to 9-week-old mice (specific pathogen-free), with body weights ranging from 21 to 23 g, were purchased from SIMM Animal Center (Shanghai, China). All animals were housed under standard laboratory conditions (21 ± 2 ℃, 12 h light-dark cycle). All animal experiments were performed based on the institutional ethical guidelines on animal care and were approved by the Institute Animal Care and Use Committee at the Shanghai Institute of Materia Medica.

The animals were fed either a control diet or MCD diet (Jiangsu Meidi Bio-pharmaceutical Co. Ltd) ad libitum for 8 weeks. At the same time, MCD-diet mice were randomized to either the pharmacological HDACi givinostat (10 mg/kg, formulated in PBS) daily or its vehicle solution by intraperitoneal (ip) injection for 8 weeks (n = 10 per group). At the end of the experiment, the mice were anesthetized with 10% chloral hydrate, and their livers were immediately harvested.

The animals were fed either an FPC diet (Jiangsu Meidi Bio-pharmaceutical Co. Ltd) plus fructose 18.9 g/L and glucose 23.1 g/L added to the drinking water, or control diet ad libitum for 16 weeks. After 6 weeks on the diet, FPC-fed mice were randomized to either

givinostat (10 mg/kg, formulated in PBS) daily or its vehicle solution by ip injection for 10 weeks (n = 10 per group). At the end of the experiment, the mice were anesthetized with 10% chloral hydrate, and their livers were immediately harvested.

Histology and immunohistochemical analysis
Liver sample was fixed in 4% paraformaldehyde, embedded in paraffin, sectioned, and stained with hematoxylin and eosin (H&E; Wuhan goodbio G1005) and Sirius red (Wuhan Goodbio G1018). For immunohistochemistry (IHC), paraformaldehyde-fixed paraffin-embedded liver sections were deparaffinized, hydrated, and stained with antibody against F4/80 (1:100, MAB5580,RD), CD68 (1:100, MAB0803, Novus), α-SMA (1:100, GB13044, RD) and Col1a1 (1:100, GB11022-1, RD). Subsequently, the slides were further processed using corresponding secondary antibodies, followed by counterstaining with hematoxylin. Sirius red stained areas and F4/80, CD68, α-SMA, and Col1a1 immunopositive areas were quantified by digital image analysis of 10 random fields per slide using the Image-Pro Plus (Media Cybernetic, Inc.). Lipid droplet accumulation in the liver was observed using Oil red O (O0625; sigma-Aldrich) staining. Frozen liver sections were stained with Oil red O staining reagent for 30 min and were counterstained with hematoxylin. To calculate the NAS score, H&E images were analyzed according to criteria described by Brunt et al. [28]. The NAS score consists of three components: steatosis, lobular inflammation, and hepatocyte ballooning.

Cell culture
The mouse macrophage cell line RAW264.7 was cultured in Dulbecco's Modified Eagle's Medium (DMEM) containing 10% heat-inactivated fetal bovine serum (Gibco, Australia) at 37 ℃, 5% CO_2 with complete media. For stimulation, the cells were treated with lipopolysaccharide (LPS) (Escherichia coli, 055:B5, Sigma, 1 μg/mL) and/or givinostat (9 μM, 3 μM, 1 μM) for 4 h or 24 h. For lipid stimulation, the cells were treated with palmitate (PA) (0.4 mM, P9767, Sigma-Aldrich) and/or givinostat (4 μM, 1 μM) for 12 h.

The human hepatocellular carcinoma cell line HepG2 and the human derived fetal hepatocyte cell line L02 were cultured in DMEM containing 10% FBS at 37 ℃, 5% CO_2 with complete media. To mimic the in vitro hepatic steatosis model, the cells were treated with PA (0.4 mM) and or givinostat (9 μM, 3 μM, 1 μM) for 12 h.

RNA-Seq analysis
Total RNA was isolated from liver tissues form control mice, vehicle treated MCD mice and givinostat-treated MCD mice. RNA Integrity Number value was used to assess the quality of the isolated RNAs. Only RNAs with RIN ≥ 7.0 were used for sequencing. The sequencing reads were located to mm10 by STAR 2.5 and the gene counting was quantified using feature counting software. The Deseq2 R package was used for differential gene expression analysis. The P value was adjusted by the Benjamini and Hochberg methods, and the 5% FDR cutoff value and the fold change greater than 1.5 were set as the threshold of the significant gene. The differentially expressed genes were further analyzed by gene-annotation enrichment analysis using the KOBAS3.0 bioinformatics platform.

RNA extraction and RT-qPCR
Total RNA was isolated with the total RNA extraction reagent (Vazyme, China) from liver tissues and cells, and then reverse transcribed with the special cDNA synthesis kit (Vazyme, China) according to the manufacturer's protocol. Quantification of gene expression was measured by RT-qPCR on Quant Studio 6 Flex Real-Time PCR system (ABI). Target genes expression was calculated using the ΔΔCt method and expression was normalized with GAPDH expression levels. The primer sequences are listed in Supplementary Table 1.

Givinostat attenuates NASH and liver fibrosis
HM Huang et al.

943

Western blotting

Total protein was extracted from RAW264.7 cells and frozen liver tissues with RIPA lysis buffer. BCA Protein Assay Kit (Sangon Biotech, China) was used to measure protein concentrations. Protein samples were separated by sodium dodecyl sulfate (SDS)-PAGE and transferred onto a nitrocellulose membrane (Millipore, Temecula, CA, USA). After blocked with 5% non-fat powdered milk, the nitrocellulose membrane was incubated with primary antibodies at 4 °C overnight, followed by incubation with the corresponding secondary antibodies for 1 h at room temperature. A ChemiScope3400 imaging system was used for signal detection. Protein expression levels were quantified by ImageJ and normalized to levels of GAPDH. The following primary antibodies were used: anti-α-SMA (Cell Signaling Technology, 19245S, 1:1000), anti-Col1a1 (Cell Signaling Technology, 39952S, 1:1000), anti-H3 (Cell Signaling Technology, 4499S, 1:1000), anti-ac-lysine (Cell Signaling Technology, 6952S, 1:1000), and GAPDH (Cell Signaling Technology, 5174S, 1:5000).

Biochemical analysis

Serum aspartate aminotransferase (AST), alanine aminotransferase (ALT), and alkaline phosphatase (ALP) were assessed using a Hitachi 7020 automatic analyzer (Hitachi, Tokyo, Japan).

ELISA

The concentration of IL-1β, IL-6, and TNF-α in RAW264.7 cells culture supernatants was analyzed using ELISA kits (No. EMIL6RA, 88-7324-22, bms6002; Thermo Scientific) according to the manufacturer's instructions.

Liver TG, TC, and intracellular TG levels quantification

Liver TG and TC levels were measured from mouse liver homogenates. The intracellular TG content was measured in HepG2 or L02 cells. Briefly, for TG quantification, wet liver tissue (100 mg) or cells (1×10^7) were homogenized in a 5% NP-40 solution. Triglyceride Quantification Kit (Sigma-Aldrich, MAK266) was used for the assay according to manufacturer's instructions. Photometric absorbance was read at 570 nm using microplate reader (Thermo Scientific, Multiskan FC). For liver TC quantification, 10 mg wet liver tissue was homogenized in a chloroform: isopropanol: IGEPAL CA-630 solution. Cholesterol Quantitation Kit (Sigma-Aldrich, MAK043) was used for the assay according to manufacture's instruction. Photometric absorbance was read at 570 nm using microplate reader (Thermo Scientific, Multiskan FC).

Statistical analysis

All results were expressed as mean ± SD, and the differences between groups were performed using GraphPad Prism 7.0 statistical software (GraphPad Software, Inc., La Jolla, CA, USA). $P < 0.05$ was considered significant.

RESULTS

Givinostat inhibited LPS and PA-induced inflammation in vitro and alleviated MCD-induced liver inflammation in vivo

Our previous high-throughput screening identified givinostat as one of the most potent inhibitors that reduced macrophage inflammatory activation. Given the crucial role of inflammation in NASH progression, we aimed to test whether givinostat could reduce liver inflammation and fibrosis, and evaluate its therapeutic efficacy for treatment of NASH. We first confirmed its anti-inflammatory effects in vitro. RAW264.7 cells were stimulated by LPS in the presence of givinostat to examine effect of givinostat on LPS-induced cytokine expression, which is indicative of macrophage inflammatory activation. We cultured RAW264.7 cells in the presence or absence of givinostat and treated them with LPS (1 μg/mL) for 4 or 24 h. RT-qPCR was used to detect the

mRNA expression levels of IL-6, IL-1β, and TNF-α, which are representative inflammatory mediators that correlated with severity of inflammation response. Data showed that LPS induced a significant increase in the mRNA and protein expression levels of IL-6, IL-1β, and TNF-α (Fig. 1a, b). Treatment with givinostat abrogated the LPS-induced transcription of these cytokines in a concentration-dependent manner (Fig. 1a). Consistently, givinostat treatment decreased the protein expression and secretion of IL-6, IL-1β, and TNF-α induced by LPS stimulation (Fig. 1b), as shown by ELISA analysis of cell supernatant. When exposed to palmitic acid (PA), RAW264.7 cells had up-regulated production of proinflammatory mediators including IL-6, IL-1β, and TNF-α. Givinostat significantly dampened PA-induced transcription of proinflammatory mediators (Fig. 1c). Notably, givinostat administration increased protein levels of acetylated Histone 3 and 4 in RAW264.7 cells (Fig. 1d), validating its on-target inhibition of HDAC.

Given the dramatic reduction of inflammation by givinostat we observed in vitro, we examined whether givinostat could also alleviate hepatic inflammation in vivo in MCD-fed mice. To determine whether givinostat affected inflammation, we examined the expression of cytokines and chemokines in livers from both givinostat-treated and vehicle-treated mice. In the livers of MCD-fed mice, concentrations of the inflammatory mediators including IL-6, TNF-α, MCP-1 (also known as CCL2), CCL5, IL-1β, CCR2, and CXCL2 were significantly higher compared to control diet-fed mice (Fig. 1e). MCD-fed mice were treated with either givinostat (10 mg/kg) daily by intraperitoneal (ip) injection or its vehicle. Expression of these inflammatory cytokines in the livers of givinostat-treated mice was reduced in comparison to that of vehicle-treated mice after 8 weeks on MCD diet (Fig. 1e). During hepatic inflammation, activated macrophages secreted CCL2 and CCL5, which recruited monocyte to the liver and further exaggerated/deteriorated liver inflammation. Recruitment of monocyte and its differentiation into inflammatory macrophage is an important step for NASH progression. The inhibition of CCL2 and CCL5 expression by givinostat in vitro and in vivo prompted us to examine whether givinostat intervention could inhibit macrophages infiltration in liver of MCD mice by performing immunohistochemical (IHC) staining of liver tissues. Results showed that macrophages marked by F4/80 and CD68 increased in the liver of MCD diet-fed mice compared with the control mice, and were significantly reduced after givinostat treatment (Fig. 1f). Taken together, these data demonstrated that givinostat treatment significantly reduced liver inflammation and infiltration of inflammatory cells in vivo in MCD-fed mice.

Givinostat protected against MCD-induced liver fibrosis

The liver inflammation is an important driving force of disease progression, as it promotes sustained liver fibrogenesis. We next examined whether givinostat could also alleviate liver fibrosis in MCD-fed mice. Sirius Red staining is commonly used to visually assess collagen levels associated with liver fibrosis. MCD-fed mice developed significant liver fibrosis as demonstrated by increased collagen deposition measured by Sirius Red staining, whilst, givinostat-treated mice showed impressively reduced amounts of collagen fibers compared with vehicle-treated mice (Fig. 2a). Morphometric analysis yielded concordant results where the Sirius Red- stained collagen areas were significantly reduced in givinostat-treated mice compared to vehicle-treated mice ($P < 0.05$) (Fig. 2a). Consistently, IHC staining of α-SMA and collagen type1 (Col1a1), the most abundant ECM protein in the fibrotic liver tissue, demonstrated that givinostat notably attenuated increased expression of α-SMA and Col1a1 in the liver of MCD-fed mice compared to vehicle-treated mice (Fig. 2b). Consistently, givinostat reduced mRNA expression of Col1a1 and α-SMA in the liver of MCD-fed mice (Fig. 2c). Furthermore, the liver Col1a1 and α-SMA
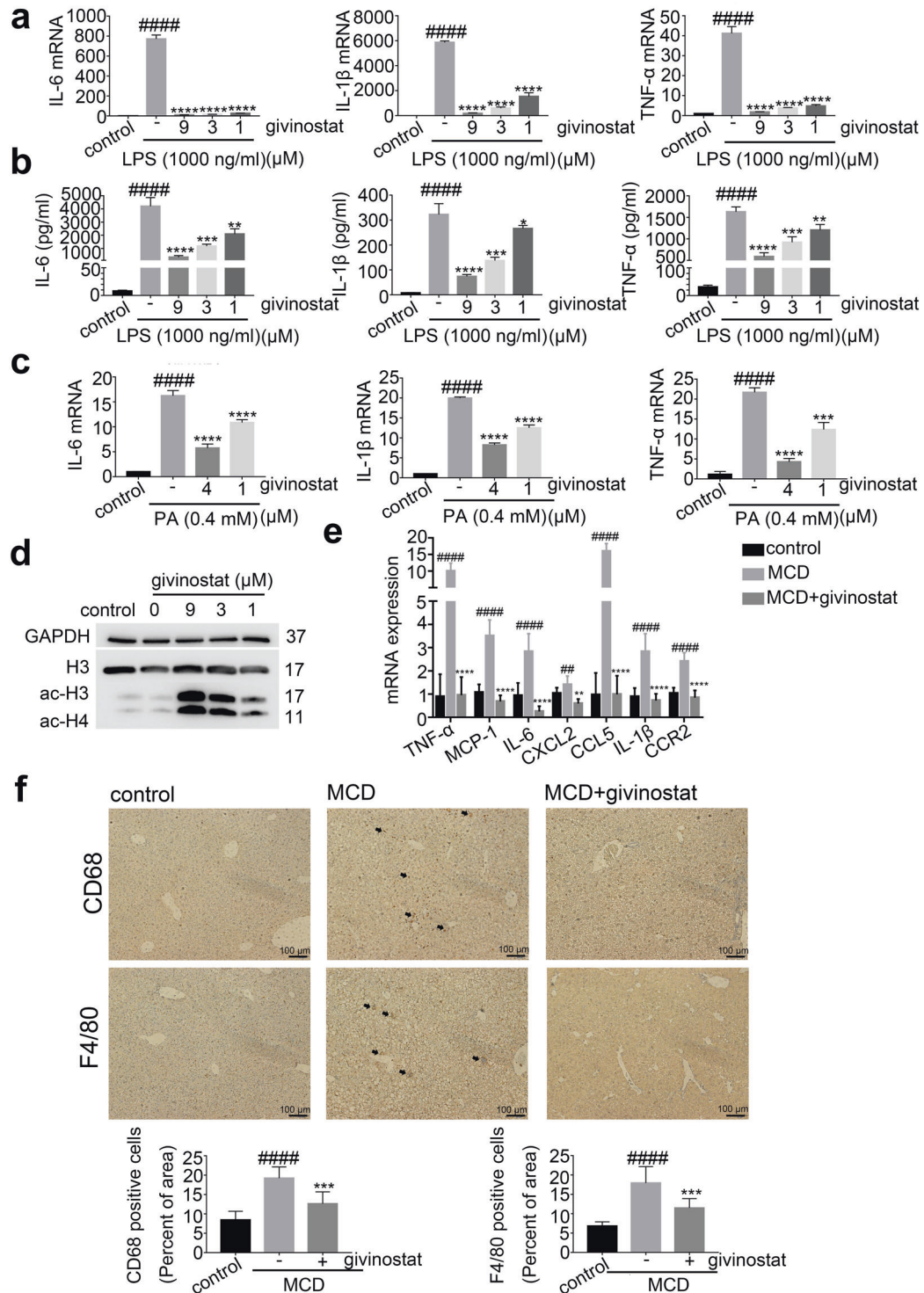
Givinostat attenuates NASH and liver fibrosis
HM Huang et al.

944

Fig. 1 Givinostat inhibited LPS and PA-induced inflammation in vitro and alleviated MCD-induced liver inflammation in vivo. a RAW264.7 cells were treated with LPS and givinostat for 4 h, after which the IL-6, IL-1β and TNF-α mRNAs were quantified by RT-qPCR analysis. **b** RAW264.7 cells were treated with LPS and givinostat for 24 h, and then the IL-6, IL-1β, and TNF-α concentrations in culture supernatants were determined by ELISA. **c** RAW264.7 cells were treated with PA and givinostat for 12 h, after which the IL-6, IL-1β, and TNF-α mRNA were quantified by RT-qPCR analysis. **d** RAW264.7 cells were treated with LPS and givinostat for 4 h, the acetylated H3 and H4 protein levels were quantified by Western blot analysis. **e** mRNA levels for genes involved in inflammation in the liver of mice were fed either chow or MCD diet for 8 weeks, and givinostat or vehicle was given simultaneously. ($n = 10$ mice per group). **f** Representative F4/80 and CD68 IHC staining and their quantification in the liver of mice were fed either chow or MCD diet for 8 weeks, and givinostat or vehicle was given simultaneously. ($n = 10$ samples from 10 mice per group). Bars represent mean ± SD. $^{\#\#}P < 0.01$, $^{\#\#\#\#}P < 0.0001$ versus control or control diet-fed mice. $^{**}P < 0.01$, $^{***}P < 0.001$, $^{****}P < 0.0001$ versus LPS or PA group or vehicle-treated MCD-fed mice.
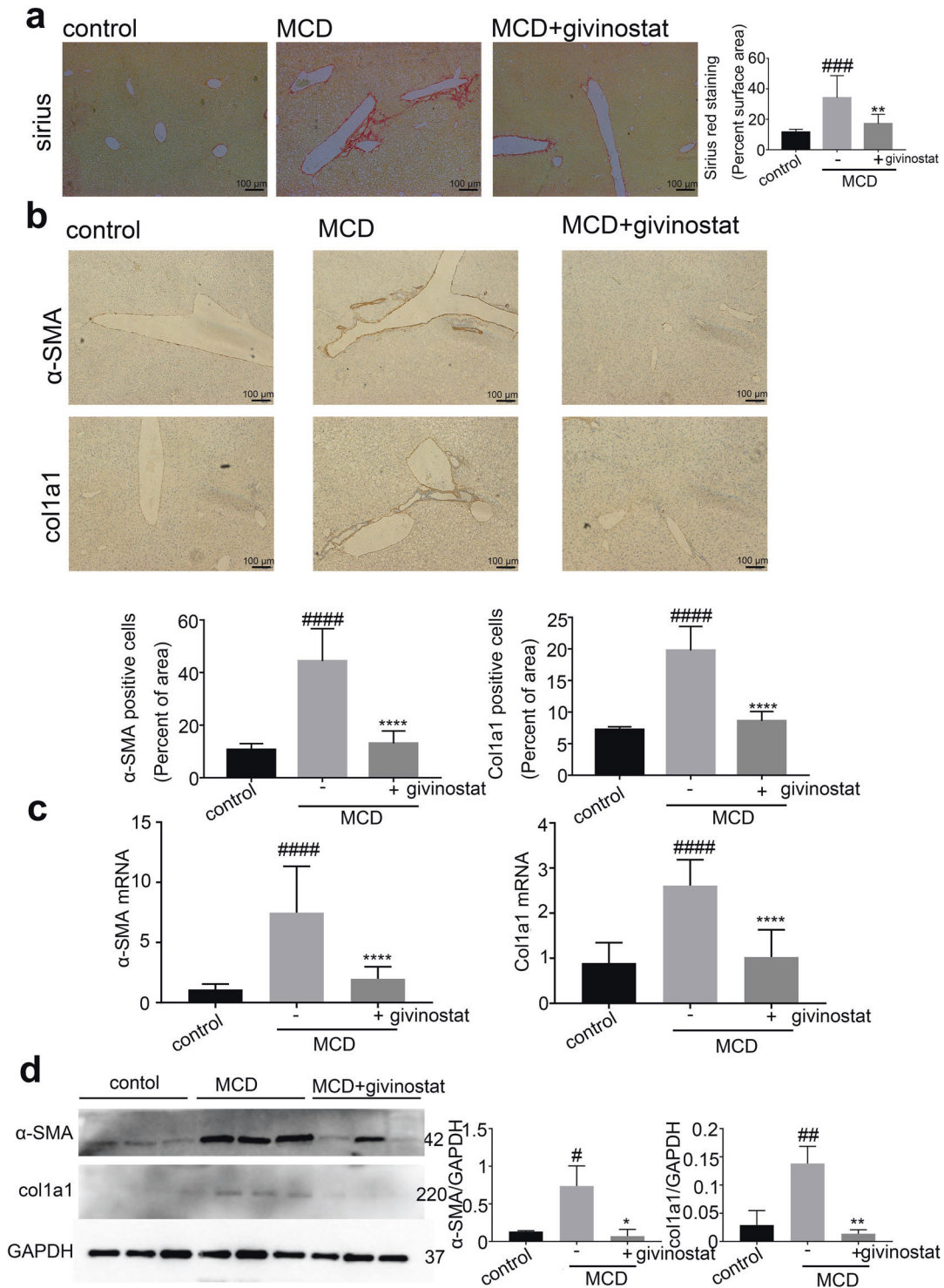
Givinostat attenuates NASH and liver fibrosis
HM Huang et al.

945

Fig. 2 **Givinostat protected against MCD-induced liver fibrosis.** C57BL/6J mice were fed either chow or MCD diet for 8 weeks, and givinostat or vehicle was given simultaneously. **a** Collagen deposition by Sirius Red staining of livers sections and their quantification shown in the right panel ($n = 10$ samples from 10 mice per group). **b** Representative Col1a1 and α-SMA IHC staining, and their quantification shown in the lower panel ($n = 10$ samples from 10 mice per group). **c** Representative RT-qPCR analysis of liver Col1a1 and α-SMA mRNA expression. **d** Representative Western blot analysis of the liver Col1a1 and α-SMA protein expression, with quantification shown in the right panel ($n = 10$ mice per group). Bars represent mean ± SD. $^{\#}P < 0.05$, $^{\#\#}P < 0.01$, $^{\#\#\#}P < 0.001$, $^{\#\#\#\#}P < 0.0001$ versus control diet-fed mice. $^{*}P < 0.05$, $^{**}P < 0.01$, $^{***}P < 0.001$, $^{****}P < 0.0001$ versus vehicle-treated MCD-fed mice

protein expression levels were also markedly reduced compared with that in vehicle-treated MCD-fed mice (Fig. 2d). Collectively, these data indicated that givinostat significantly alleviated liver fibrosis in the MCD-fed mice.

Givinostat regulated inflammatory and metabolism gene expression in vivo as determined by RNA-Seq analysis
Next we investigated the mechanism underlying the therapeutic efficacy of givinostat. RNA sequencing (RNA-seq) analysis was

Givinostat attenuates NASH and liver fibrosis
HM Huang et al.

946

performed to compare the gene expression profiles of liver tissues from control mice, vehicle treated MCD mice and givinostat-treated MCD mice, followed by principle component analysis (PCA) and differential expression genes (DEGs) analysis. Then DEGs were analyzed by KEGG pathway enrichment. In PCA, principle component 1 (PC1) and principle component 2 (PC2) take a high proportion of variance, which means they can explain the difference between groups (Fig. 3a). Based on PC1 and PC2, three groups are classified distinctly, which means that givinostat treatment could change MCD condition (Fig. 3b). Then, we analyzed DEGs between Model group and HDACi givinostat-treated group. Then DEGs defined as P.adj < 0.05 and log2FC ≥ 1.5 were selected to undergo subsequent KEGG pathway enrichment analysis. When compared with the control group, a large number of genes were up-regulated or down-regulated upon MCD treatment, and the levels of quite a few of genes

were reversed close to the control group after givinostat treatment (Fig. 3c). The numbers of differentially expressed genes were 1093 and 941, for vehicle +MCD compared with the control group, and the givinostat +MCD compared with the control, respectively (Fig. 3d).

Consistent with above RT-qPCR data, givinostat shows its inflammation-modulating effect because several inflammatory pathways are regulated. Cytokine–cytokine receptor interaction pathway, inflammatory mediator regulation of TRP channel pathway and viral interaction with cytokine and cytokine receptor pathway is important in inflammatory mediator regulation.

Intriguingly, we found many enriched genes were related to metabolism regulation. Retinol metabolism pathway ranked first and some other important metabolism pathways like PPAR, steroid biosynthesis, and bile secretion followed closely (Fig. 3e). We selected several genes with the most obvious changes in the
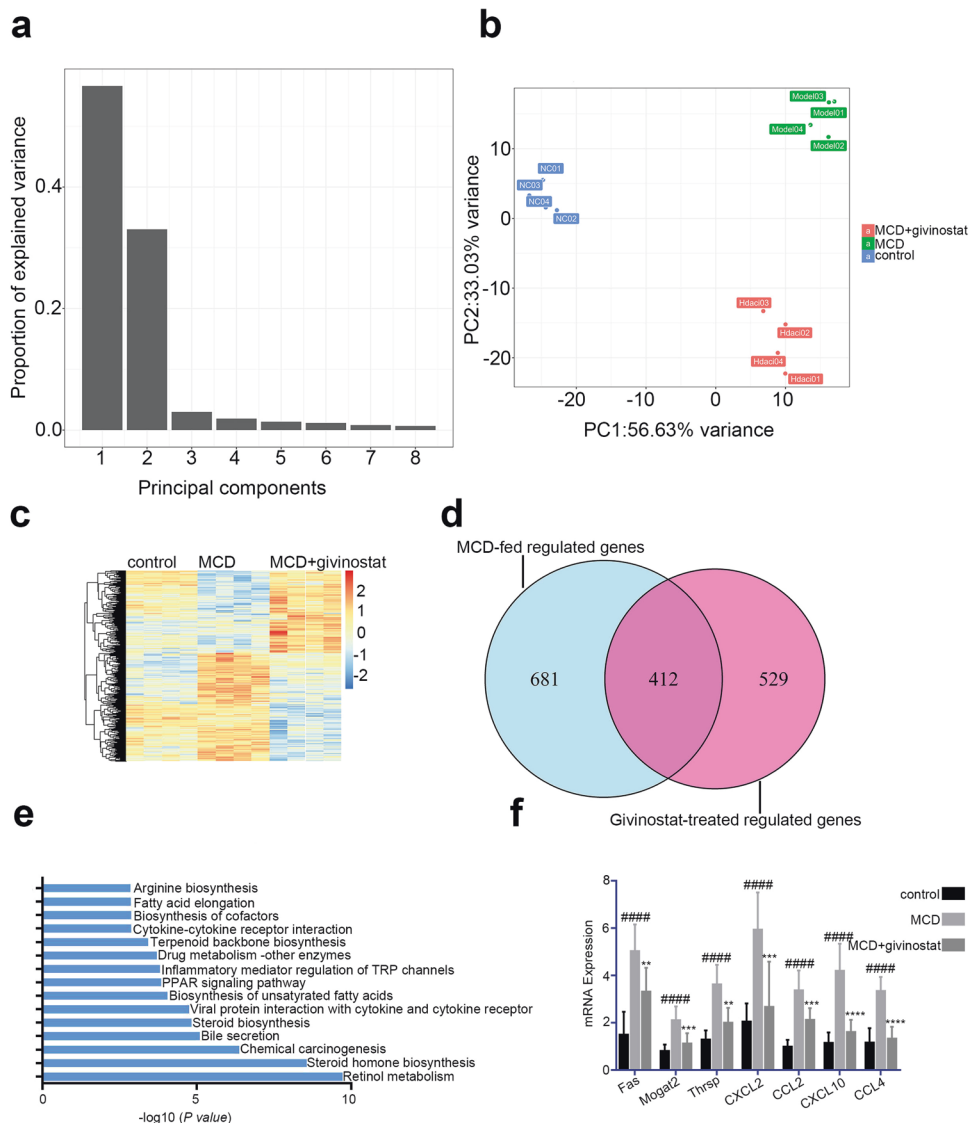

Fig. 3 Givinostat regulated inflammatory and metabolism gene expression in vivo as determined by RNA-Seq analysis. RNA-seq analysis was performed on liver tissues extracted from mice fed either chow or MCD diet for 8 weeks, and givinostat or vehicle was given simultaneously. ($n = 4$ mice per group). **a, b** Principle component analysis among three groups. **c** The heat map of genes with adjusted P value < 0.05, and absolute value of log2 fold-change > 1.5. **d** Venn diagram showing the overlap between the gene set of MCD-fed regulated genes and the gene set subsequently regulated by givinostat in vivo. **e** KEGG pathway analysis using differentially expressed genes between givinostat-treated MCD-fed and vehicle-treated mice, showing that the most significantly enriched pathways are related to the inflammatory and lipid metabolism response. **f** RT-qPCR analysis was performed to validate the repression of hub genes by givinostat ($n = 10$ mice per group). Bars represent mean ± SD. $^{####}P < 0.0001$ versus control diet-fed mice. $^{**}P < 0.01$, $^{***}P < 0.001$, $^{****}P < 0.0001$ versus vehicle-treated MCD-fed mice

Givinostat attenuates NASH and liver fibrosis
HM Huang et al.

947

expression levels of inflammation-related pathways and lipid metabolism related pathways, and detected the expression levels of these genes between vehicle-treated and givinostat-treated MCD-fed mice by RT-qPCR. Thyroid hormone responsive, mono-acylglycerol acyltransferase (mogat2) and fatty acid synthase (Fan) genes which regulate fatty acid synthesis, were significantly increased in vehicle-treated MCD-fed mice compared to control mice, givinostat-treated MCD-fed mice exhibited an opposite pattern of expression of these lipid metabolic genes in the liver compared to vehicle-treated MCD-fed mice (Fig. 3f). CXCL2, CCL2, CXCL10, and CCL4 genes which regulate inflammatory responses, were significantly increased in vehicle-treated MCD-fed mice compared to control mice. Givinostat-treated MCD-fed mice exhibited an opposite pattern of expression of these inflammatory response genes in the liver compared to vehicle-treated MCD-fed mice (Fig. 3f). From RNA-seq results, we conclude that givinostat potently blocked pathologic pro-inflammatory genes and regulated a broad set of lipid metabolism-related genes, prompting us to explore the protective effect of givinostat on hepatic steatosis.

Givinostat alleviated MCD-induced hepatic steatosis

We further elucidated the effects of givinostat on hepatic steatosis in MCD fed mice. The liver tissue of MCD mice exhibited obvious steatosis, ballooning hepatocytes, scattered lobular inflammatory cell infiltration, and inflammatory foci, as indicated by HE and Oil red O staining (Figs. 4a, 4b, middle panel). In contrast, the givinostat-treated mice showed minimal steatosis, with only a few small foci of steatosis observed in the centrilobular area (Fig. 4a, b, right panel). NASH scores further confirmed that givinostat treatment resulted in a decrease in hepatic steatosis, ballooning of hepatocytes, and inflammation compared to vehicle-treated mice (Fig. 4c). Consistently, the livers of vehicle-treated MCD-fed mice exhibited significantly increased lipid accumulation and content compared with control-fed mice, whereas the livers of givinostat-treated MCD-fed mice showed significantly reduced liver triglyceride (TG) and cholesterol (TC) levels (Fig. 4d). Moreover, RT-qPCR analysis of liver samples indicated that the mRNA expression of genes involved in fatty acid β-oxidation (cholesterol 7α-hydroxylase [CYP7A], acyl-coenzyme A oxidase 1 [ACOX-1], Cytochrome c oxidase subunit 5A [COX5A], uncoupling protein 2 [UCP2], and pyruvate dehydrogenase kinase4 [PDK4]) was greatly attenuated, whereas genes involved in cholesterol and fatty acid synthesis (Fatty acid synthase [FAS], sterolregulatory element-binding protein-1c [SREBP-1c], and stearoyl-CoA desaturase-1 [SCD1]) were significantly increased in vehicle-treated MCD-fed mice compared to control mice (Fig. 4e). Givinostat-treated MCD-fed mice exhibited an opposite pattern of expression of these lipid metabolic genes in the liver compared to vehicle-treated MCD-fed mice (Fig. 4e). In addition, the plasma levels of ALT and AST, major markers of liver function, were elevated in vehicle-treated MCD-fed mice compared with control mice. Givinostat treatment significantly reduced serum AST and ALT activity in MCD-fed mice (Fig. 4f), suggesting alleviated liver damage. Together, these findings demonstrate that givinostat treatment inhibited hepatic hepatosis, inflammation as well as fibrosis in MCD mice, thus improving NASH score and alleviating liver injury.

Givinostat diminished PA-induced intracellular lipid accumulation in hepatocytes

Givinostat alleviated hepatic steatosis and regulated a broad set of lipid metabolic genes. We next examined whether givinostat directly affected lipid accumulation in hepatocyte in vitro. We used a PA-induced in vitro fatty liver cell model. We induced lipid accumulation in hepatic cells by exposing them to PA, to simulate excessive influx of free fatty acids into hepatocytes. The experiments were performed using PA complexed with bovine

serum albumin (BSA) at a FFA to BSA ratio of 5.2:1 [29]. Human hepatoma cells (HepG2) and L02 cells were cultured with 0.4 mM PA for 12 h in the presence or absence of givinostat, as a control, HepG2 or L02 cells were treated with equimolar BSA carrier protein. HepG2 or L02 cells treated with 0.4 mM PA for 12 h exhibited significant increased lipid droplet accumulation compared to control cells treated with BSA, while minimal staining for lipids was seen in givinostat-treated cells, as indicated by Oil red O staining (Fig. 5a, b). The availability of FFA increases with increased intake and is expected to enhance liver TG synthesis. We measured intracellular TG content in HepG2 or L02 cells that were exposed to 0.4 mM PA for 12 h (Fig. 5c, d). Compared with the BSA control cells, PA-treated cells exhibited significantly increased lipid accumulation and content, whereas the givinostat-treated cells presented the opposite trend compared with PA-treated cells, as indicated by TG levels (Fig. 5c, d). Thus, we observed a direct inhibitory effect of givinostat on lipid accumulation in vitro.

FPC-induced liver inflammation was diminished by givinostat

Encouraged by the potent regulatory effects of givinostat on hepatocyte metabolism and inflammation, we assessed the therapeutic efficiency of givinostat for NASH treatment and examined its impact on liver inflammation and lipid metabolism using mouse NASH models induced by diet rich in fructose, palmitate, cholesterol (FPC) [30]. C57BL/6J mice were fed either chow or FPC diet for 16 weeks, and givinostat or vehicle was given during the last 10 weeks. After 16 weeks, FPC-fed mice had significantly higher serum ALT, AST, and ALP levels when compared with control diet fed mice, whereas givinostat-treated FPC-fed mice had a considerable reduction of serum ALT, AST, and ALP levels compared with vehicle-treated FPC-fed mice, reflecting reduced liver injury (Fig. 6a). IHC staining of liver tissues showed that vehicle-treated FPC-fed mice had a significant increase in macrophage (marked by F4/80 and CD68) in the liver than in liver of control diet fed mice, which was remarkably reduced by givinostat treatment (Fig. 6b). A significant increase in mRNA levels of inflammation genes, including IL-6, TNF-α, MCP-1, CCL5, IL-1β, CCR2 and CXCL2, was observed in livers of vehicle-treated FPC-fed mice compared to control diet fed mice (Fig. 6c). Relative to FPC-fed mice treated with vehicle, givinostat-treated mice exhibited a considerable reduction in inflammatory gene expression in the liver (Fig. 6c). Taken together, these data demonstrated that givinostat treatment reduced liver dysfunction and inflammatory response in FPC-diet induced NASH mice model.

FPC-induced hepatic steatosis was diminished by givinostat

We further examined whether givinostat could ameliorate steatosis in FPC-fed NASH mice. Vehicle-treated FPC-fed mice, in comparison to control diet fed mice, exhibited strikingly greater levels of steatosis, ballooning hepatocytes, scattered lobular inflammatory cell infiltration, and inflammatory foci in the liver, as indicated by HE and Oil red O staining, which were reversed by givinostat treatment (Fig. 7a, b). Consistently, givinostat treatment significantly reduced the NASH scores in FPC-fed mice (Fig. 7c). Furthermore, the livers of vehicle-treated FPC-fed mice exhibited significantly increased lipid accumulation and content compared with control diet-fed mice, whereas the livers of givinostat-treated FPC-fed mice presented the opposite trend compared with vehicle-treated FPC-fed mice, as indicated by liver TG and TC levels (Fig. 7d). Moreover, RT-qPCR analysis of liver samples indicated that the mRNA expression of genes involved in fatty acid β-oxidation (CYP7A, ACOX-1, COX5A, UCP2, and PDK4) were greatly attenuated, whereas cholesterol and fatty acid synthesis (FAS, SREBP-1c, and SCD1) were significantly increased in vehicle-treated FPC-fed mice compared to control mice (Fig. 7e). However, givinostat-treated FPC-fed mice exhibited an opposite pattern of
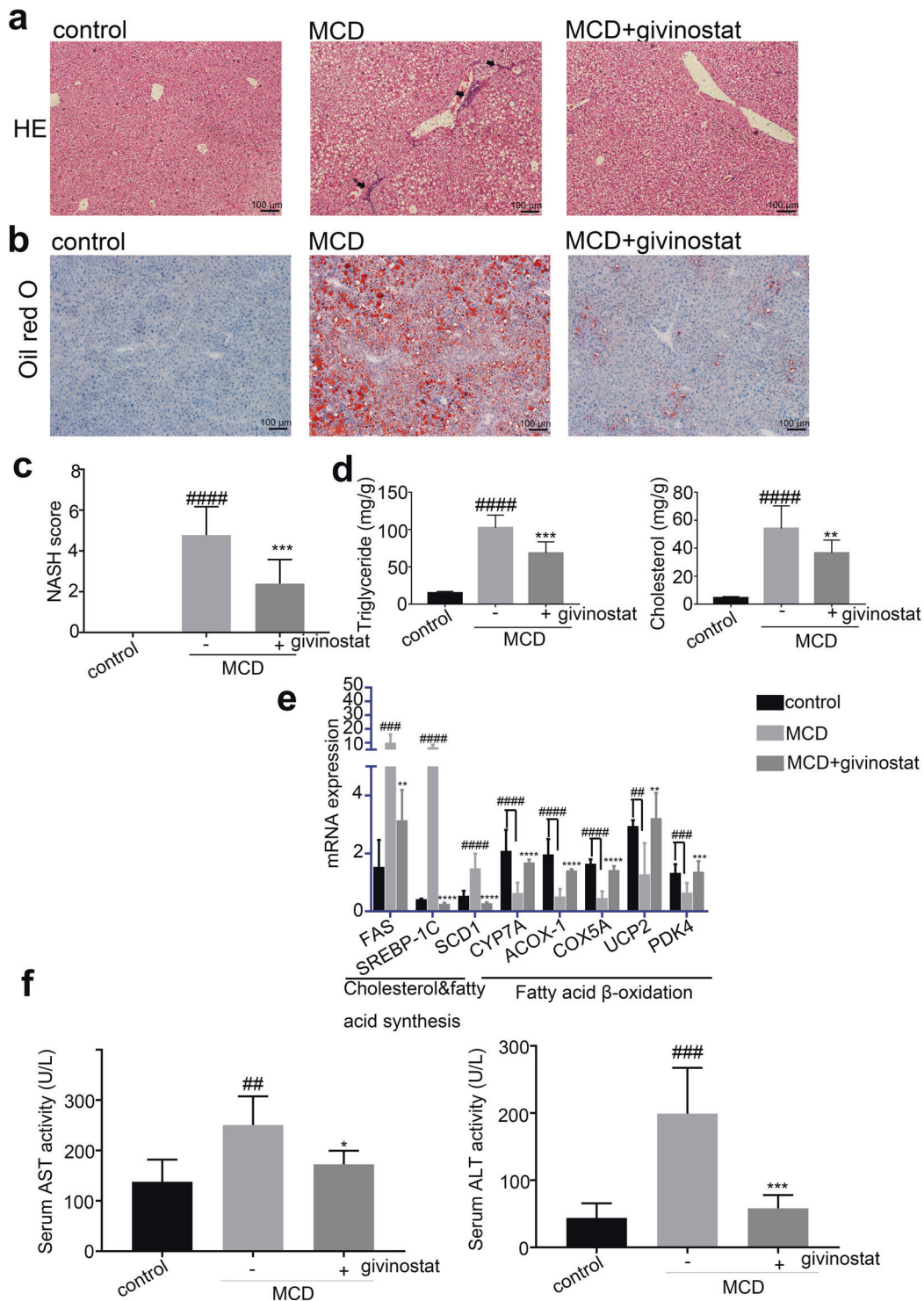
Givinostat attenuates NASH and liver fibrosis
HM Huang et al.

948

Fig. 4 Givinostat alleviated MCD-induced hepatic steatosis. C57BL/6J mice were fed either chow or MCD diet for 8 weeks, and givinostat or vehicle was given simultaneously. **a** Representative images of HE stained liver sections. **b** Representative images of Oil Red O stained liver sections. **c** The NASH scores ($n = 10$ mice per group). **d** The TG and TC levels in the livers ($n = 10$ mice per group). **e** Transcript levels of lipid metabolism-related genes in the livers ($n = 10$ mice per group). **f** The plasma AST and ALT levels in mice ($n = 10$ mice per group). Bars represent mean ± SD. $^{##}P < 0.01$, $^{###}P < 0.001$, $^{####}P < 0.0001$ versus control diet-fed mice. $^{*}P < 0.05$, $^{**}P < 0.01$, $^{***}P < 0.001$, $^{****}P < 0.0001$ versus vehicle-treated MCD-fed mice

expression of these lipid metabolic genes in the liver compared to vehicle-treated FPC-fed mice. Together, givinostat resulted in remarkable reduction in hepatic inflammation, lipid accumulation and liver dysfunction, as well as a significant improvement in fatty acid synthesis and oxidation in FPC-fed mice.

DISCUSSION
NAFLD is emerging as a worldwide public health threat [31]. A number of patients with NAFLD develop a more inflammatory and progressive subtype-NASH, which can lead to cirrhosis and end-edge liver disease [32, 33]. The cornerstones of NAFLD treatment

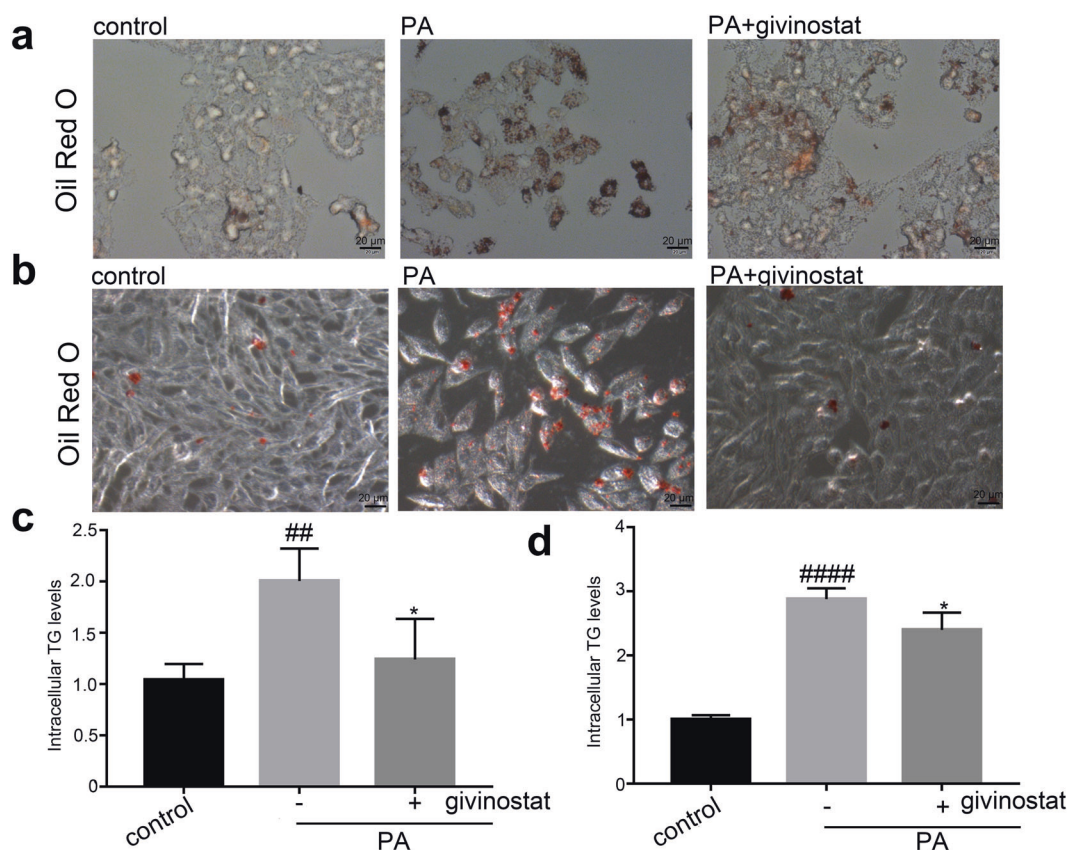Givinostat attenuates NASH and liver fibrosis
HM Huang et al.

949

Fig. 5 Givinostat diminished palmitic acid-induced intracellular lipid accumulation in hepatocytes. a Representative images of Oil Red O staining of HepG2 cells that were treated with vehicle (control) or PA for 12 h. **b** Representative images of Oil Red O staining of L02 cells that were treated with vehicle (control) or PA for 12 h. **c** The intracellular TG content in HepG2 cells after treatment with PA or vehicle for 12 h. **d** The intracellular TG content in L02 cells after treatment with PA or vehicle for 12 h. Bars represent mean ± SD. ##$P < 0.01$, ####$P < 0.0001$ versus BSA control cells. *$P < 0.05$, versus PA treated cells

are weight loss and increased amounts of exercise, but maintaining these lifestyle changes can be hard. Development of pharmacotherapy is in urgent needs when lifestyle modifications are not achieved and sustained [34]. Currently, although many clinical trials are being investigated actively, there is still a lack of efficient drug for treatment of NASH. Our current work demonstrates the efficacy of givinostat for treatment of NASH via targeting inflammation and metabolism pathways.

As histone deacetylases could erase histone acetylation marks and regulate histone and chromatin structures, HDACs are classified into four groups: class I; class II; class III known as the sirtuins, and class IV is represented by HDAC11 only [35, 36]. Givinostat is a pan-HDAC inhibitor that belongs to hydroxamic acids family, with inhibition on class I, class II and class IV HDACs [37]. Givinostat is being evaluated in phase III clinical trials at Italfarmaco company for the treatment of Duchenne's muscular dystrophy [38], and is also undergoing Phase II clinical trials related to myeloproliferative diseases or polycythemia vera [Clinical trial NCT01901432]. Considering the crucial role of inflammation in NASH disease progression, we identified givinostat as a potent anti-inflammatory compound and assessed its pharmacologic efficacy for treatment of NASH. We found givinostat inhibited LPS and PA-induced macrophage inflammatory activation in vitro, alleviated inflammatory cytokines expression and inflammatory cell infiltration in liver in NASH animal models. Our previous study also showed that givinostat inhibited HSC activation and alleviated fibrogenesis in CCl₄-induced liver fibrosis mouse model, which is consistent with other reports. The anti-inflammatory and anti-fibrogenesis roles of givinostat have been revealed in several acute liver disease models, yet whether

HDAC inhibitors could alleviate inflammation and fibrosis in chronic disease requires further study. Recent studies have demonstrated that givinostat could interfere inflammation and fibrosis progression in different diseases like intestinal epithelial inflammation or osteoarthritis [39, 40]. This prompted us to examine whether givinostat could serve as a potential candidate for treatment of NASH, which remains undetermined up to now. Our study employed two models of NASH, MCD and FPC diets, to study the pharmacological potential of givinostat for treatment of NASH. MCD diet induced liver inflammation and fibrosis, but lacked certain characteristics of human NASH pathology (like obesity or insulin resistance). FPC diet induced a phenotype of obesity, steatosis and steatohepatitis, resembling human NAFLD pathology, but lacked severe fibrosis. So we used both models and demonstrated the beneficial effects of givinostat in ameliorating hepatic steatosis, inflammation, and fibrosis.

The RNA-seq and mechanistic data suggest that givinostat regulated pathways related to steatosis, inflammation and fibrosis. Its multiple involvements in pathways protecting against NASH, may imply pleiotropic aspects of givinostat. The pathogenesis of NASH is complex and includes a complicated molecular network. Strategies targeting a single step might not lead to a satisfying outcome [41]. Drugs targeting different steps of NASH pathogenesis have been developed and tested in clinical trial. Lipid-lowering agents like Stearoyl-CoA Desaturase (SCD1) inhibitors [42] or Thyroid Hormone Receptor agonists [43] are aimed at modulating metabolism and lipid steatohepatitis. In addition to these, antidiabetic agents and antiobesity agents are also promising candidates [44, 45]. Considering the progression of NAFLD and NASH, there are some other agents involved in anti-
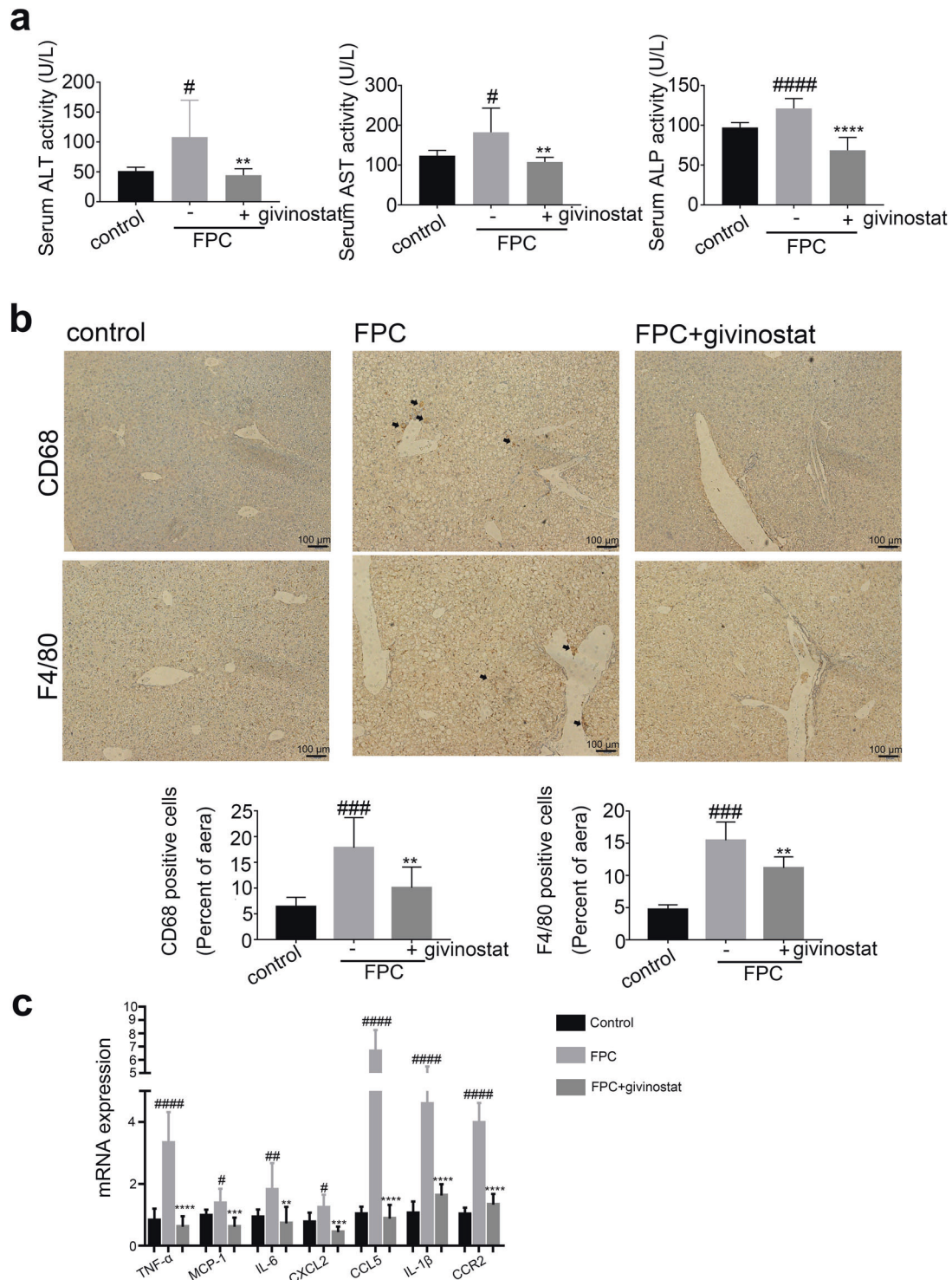
Givinostat attenuates NASH and liver fibrosis
HM Huang et al.

950

Fig. 6 FPC-induced liver inflammation was diminished by givinostat. C57BL/6J mice were fed either chow or FPC diet for 16 weeks, and givinostat or vehicle was given during the last 10 weeks. **a** The plasma ALT, AST and ALP levels in mice ($n = 10$ mice per group). **b** Representative F4/80 and CD68 IHC staining and their quantification ($n = 10$ samples from 10 mice per group). **c** mRNA levels for genes involved in inflammation in the liver ($n = 10$ mice per group). Bars represent mean ± SD. $^{\#}P < 0.05$, $^{\#\#}P < 0.01$, $^{\#\#\#}P < 0.001$, $^{\#\#\#\#}P < 0.0001$ versus control diet fed mice. $^{**}P < 0.01$, $^{***}P < 0.001$, $^{****}P < 0.0001$ versus vehicle-treated FPC-fed mice

inflammatory and antifibrotic pathways. Among these, targeting Farnesoid X Receptor [46], Obeticholic acid is in pre-registered condition. Drugs targeting chemokine receptors [47] and ASK1 are also being investigated [48]. The current status of various clinical pipelines is consistent with complex pathogenesis of NAFLD and NASH. However, it is inconclusive that therapeutic treatment should intervene with which step. Drugs targeting single step or specific targets of NASH turn out to be disappointing in clinic, thus it is proposed that combinatory therapies targeting multiple disease drivers might result in more satisfying results. Givinostat achieves its therapeutic potential for NASH by simultaneously modulating lipid metabolic dysfunction while decreasing
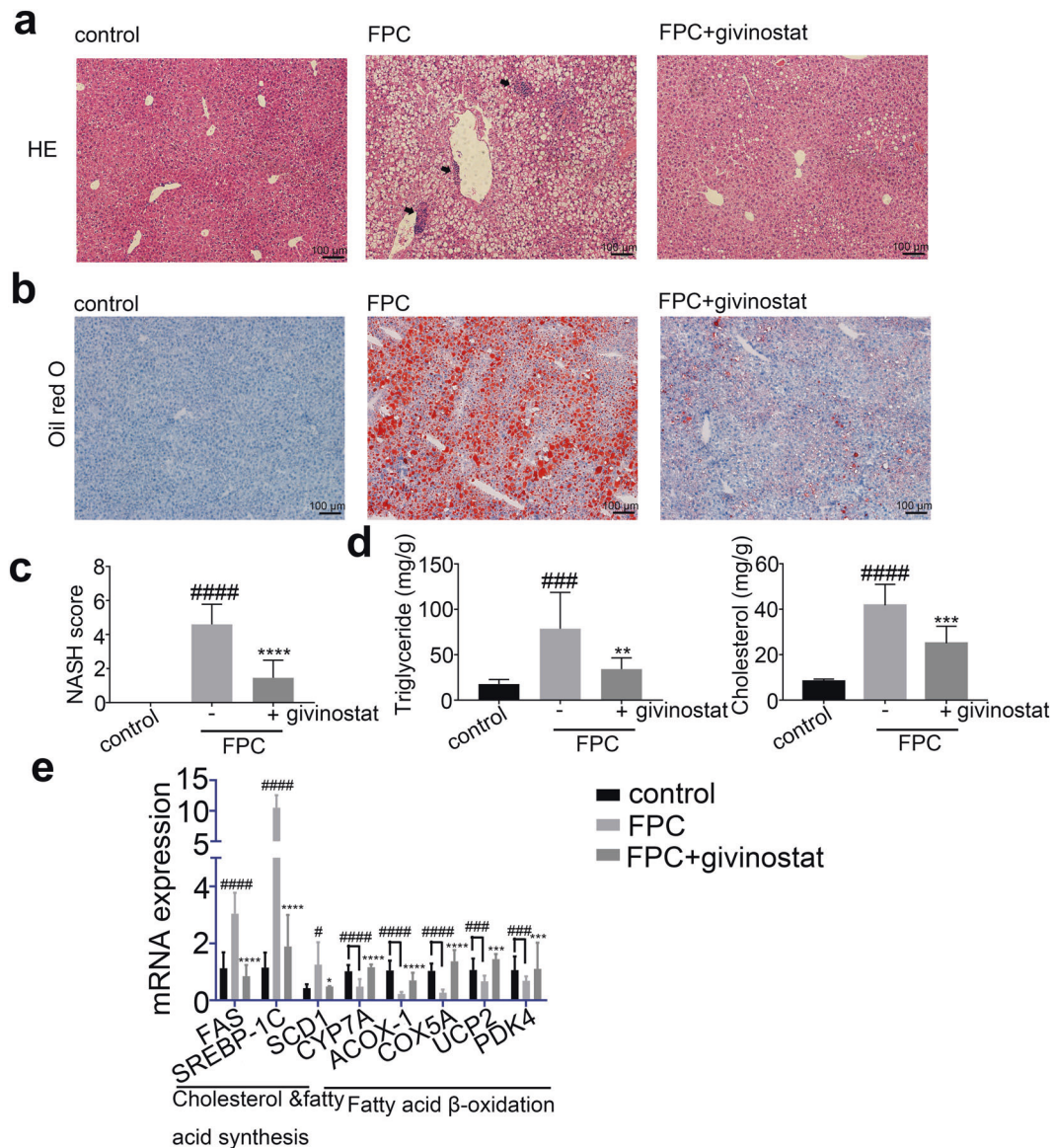
Givinostat attenuates NASH and liver fibrosis
HM Huang et al.

951

Fig. 7 FPC-induced hepatic steatosis was diminished by givinostat. C57BL/6J mice were fed either chow or FPC diet for 16 weeks, and givinostat or vehicle was given during the last 10 weeks. **a** Representative images of HE stained liver sections. **b** Representative images of Oil Red O stained liver sections. **c** The NASH scores ($n = 10$ mice per group). **d** The TG and TC levels in the livers ($n = 10$ mice per group). **e** Transcript levels of lipid metabolism-related genes in the livers ($n = 10$ mice per group). Bars represented mean ± SD. #$P < 0.05$, ###$P < 0.001$, ####$P < 0.0001$ versus control diet-fed mice. *$P < 0.05$, ***$P < 0.001$, ****$P < 0.0001$ versus vehicle-treated FPC-fed mice

inflammation and fibrosis, making it an attractive drug for treatment of NASH but also a potential complementary partner for novel combination therapies.

Beyond givinostat's anti-inflammation and anti-fibrogenesis effect, transcriptomic analysis revealed that givinostat significantly reduced expression of diverse metabolic genes. KEGG pathway enrichment analysis revealed that the major hepatic transcriptional signature affected by givinostat was associated with lipid metabolism pathways like PPAR signaling pathway or lipid biosynthesis pathways. In support of our findings, studies in hepatic cell in vitro suggested that givinostat could diminish PA-induced intracellular lipid accumulation. In past reports, inhibiting class I HDACs could prompt adipocytes differentiation to oxidative phenotype by regulating *Pparg* and *Ucp1* genes [49]. Meanwhile, report shows that through disruption of the class IIa HDAC corepressor complex, whole-body energy expenditure and lipid oxidation could be increased [50]. Our findings together with these clues indicate that epigenetic mechanism may participate in

regulation of metabolism especially lipid homeostasis. Moreover, bromodomain extraterminal domain proteins, another important epigenetic targets which are related to histone modification reading, have been reported to be involved in lipid biosynthesis, uptake and intracellular trafficking [51]. These indicated that drugs targeting epigenetic proteins could share extended indications in the treatment of metabolic disorder diseases.

In summary, givinostat potently alleviated diet-induced hepatic steatosis, inflammation as well as liver injury and fibrosis. Mechanically, givinostat inhibited expression of pathological pro-inflammatory genes as well as regulated a broad set of genes related to lipid metabolism. Givinostat could also directly inhibit HSCs activation and expression of ECM proteins in vitro. NASH is a complex, multifactorial disease, and is driven by multiple mechanisms including hepatic lipo-toxicity, inflammation, and fibrosis. Givinostat alleviated NASH by targeting multiple aspects crucial for NASH progression, suggesting the repurposing givinostat for treatment of NASH.

Givinostat attenuates NASH and liver fibrosis
HM Huang et al.

952

AUTHOR CONTRIBUTIONS

HMH, YJL, RF, LY and SJF performed immunofluorescence, Western-blot analysis, and NASH experiments, analyzed data, and wrote the manuscript. XRZ, JH, XL, LPL and SJF contributed to manuscript revising, and analyzed the RNA-seq data. GML, CL, CCS, JGF and YYZ conceived and supervised the project and revised the manuscripts.

ADDITIONAL INFORMATION

Supplementary information The online version contains supplementary material available at https://doi.org/10.1038/s41401-021-00725-1.

Competing interests: The authors declare no competing interests.

REFERENCES

1. Younossi ZM, Koenig AB, Abdelatif D, Fazel Y, Henry L, Wymer M. Global epidemiology of nonalcoholic fatty liver disease-meta-analytic assessment of prevalence, incidence, and outcomes. Hepatology. 2016;64:73–84.
2. Younossi ZM, Blissett D, Blissett R, Henry L, Stepanova M, Younossi Y, et al. The economic and clinical burden of nonalcoholic fatty liver disease in the United States and Europe. Hepatology. 2016;64:1577–86.
3. Estes C, Razavi H, Loomba R, Zobair Y, Sanyal AJ. Modeling the epidemic of nonalcoholic fatty liver disease demonstrates an exponential increase in burden of disease. Hepatology. 2018;67:123–33.
4. Estes C, Anstee QM, Arias-Loste MT, Bantel H, Bellentani S, Caballeria J, et al. Modeling NAFLD disease burden in China, France, Germany, Italy, Japan, Spain, United Kingdom, and United States for the period 2016–2030. J Hepatol. 2018; 69:896–904.
5. Wree A, Broderick L, Canbay A, Hoffman HM, Feldstein AE. From NAFLD to NASH to cirrhosis-new insights into disease mechanisms. Nat Rev Gastroenterol Hepatol. 2013;10:627–36.
6. Mikolasevic I, Filipec-Kanizaj T, Mijic M, Jakopcic I, Milic S, Hrstic I, et al. Non-alcoholic fatty liver disease and liver transplantation—where do we stand? World J Gastroenterol. 2018;24:1491–506.
7. Miura K, Yang L, van Rooijen N, Ohnishi H, Seki E. Hepatic recruitment of macrophages promotes nonalcoholic steatohepatitis through CCR2. Am J Physiol Gastrointest Liver Physiol. 2012;302:G1310–G1321.
8. Itoh M, Suganami T, Kato H, Kanai S, Shirakawa I, Sakai T, et al. CD11c+ resident macrophages drive hepatocyte death-triggered liver fibrosis in a murine model of nonalcoholic steatohepatitis. JCI Insight. 2017;16:e92902.
9. Koyama Y, Brenner DA. Liver inflammation and fibrosis. J Clin Invest. 2017;127: 55–64.
10. Seki E, De Minicis S, Osterreicher CH, Kluwe J, Osawa Y, Brenner DA, et al. TLR4 enhances TGF-beta signaling and hepatic fibrosis. Nat Med. 2007;13:1324–32.
11. Sanyal AJ. Past, present and future perspectives in nonalcoholic fatty liver disease. Nat Rev Gastroenterol Hepatol. 2019;16:377–86.
12. Ramachandran P, Iredale JP. Macrophages: central regulators of hepatic fibrogenesis and fibrosis resolution. J Hepatol. 2012;56:1417–9.
13. Pradere J-P, Kluwe J, De Minicis S, Jiao J-J, Gwak G-Y, Dapito DH, et al. Hepatic macrophages but not dendritic cells contribute to liver fibrosis by promoting the survival of activated hepatic stellate cells in mice. Hepatology. 2013;58:1461–73.
14. Miura K, Kodama Y, Inokuchi S, Schnabl B, Aoyama T, Ohnishi H, et al. Toll-like receptor 9 promotes steatohepatitis by induction of interleukin-1beta in mice. Gastroenterology. 2010;139:323–34.
15. Huang W, Metlakunta A, Dedousis N, Zhang P, Sipula I, Dube JJ, et al. Depletion of liver Kupffer cells prevents the development of diet-induced hepatic steatosis and insulin resistance. Diabetes. 2010;59:347–57.
16. Neyrinck AM, Cani PD, Dewulf EM, De Backer F, Bindels LB, Delzenne NM. Critical role of Kupffer cells in the management of diet-induced diabetes and obesity. Biochem Biophys Res Commun. 2009;385:351–6.
17. Seki E, de Minicis S, Inokuchi S, Taura K, Miyai K, van Rooijen N, et al. CCR2 promotes hepatic fibrosis in mice. Hepatology. 2009;50:185–97.
18. Seki E, De Minicis S, Gwak G-Y, Kluwe J, Inokuchi S, Bursill CA, et al. CCR1 and CCR5 promote hepatic fibrosis in mice. J Clin Invest. 2009;119:1858–70.
19. Berres M-L, Koenen RR, Rueland A, Zaldivar MM, Heinrichs D, Sahin H, et al. Antagonism of the chemokine Ccl5 ameliorates experimental liver fibrosis in mice. J Clin Invest. 2010;120:4129–40.
20. Friedman S, Sanyal A, Goodman Z, Lefebvre E, Gottwald M, Fischer L, et al. Efficacy and safety study of cenicriviroc for the treatment of non-alcoholic steatohepatitis in adult subjects with liver fibrosis: CENTAUR Phase 2b study design. Contemp Clin Trials. 2016;47:356–65.
21. Musso G, Cassader M, Gambino R. Non-alcoholic steatohepatitis: emerging molecular targets and therapeutic strategies. Nat Rev Drug Discov. 2016;15:249–74.
22. Zimmer V, Lammert F. Genetics and epigenetics in the fibrogenic evolution of chronic liver diseases. Best Pract Res Clin Gastroenterol. 2011;25:269–80.
23. Brunt EM, Wong VWS, Nobili V, Day CP, Sookoian S, Maher JJ, et al. Nonalcoholic fatty liver disease. Nat Rev Dis Prim. 2015;1:15080.
24. Fan Z, Li L, Li M, Zhang X, Hao C, Yu L, et al. The histone methyltransferase Suv39h2 contributes to nonalcoholic steatohepatitis in mice. Hepatology. 2017;65:1904–19.
25. Horsburgh S, Robson-Ansley P, Adams R, Smith C. Exercise and inflammation-related epigenetic modifications: focus on DNA methylation. Exerc Immunol Rev. 2015;21:26–41.
26. Alam R, Abdolmaleky HM, Zhou JR. Microbiome, inflammation, epigenetic alterations, and mental diseases. Am J Med Genet B Neuropsychiatr Genet. 2017; 174:651–60.
27. Peng JJ, Li JC, Huang J, Xu P, Huang HH, Liu YJ, et al. p300/CBP inhibitor A-485 alleviates acute liver injury by regulating macrophage activation and polarization. Theranostics. 2019;9:8344–61.
28. Brunt EM, Kleiner DE, Wilson LA, Belt P, Neuschwander-Tetri BA. Nonalcoholic fatty liver disease (NAFLD) activity score and the histopathologic diagnosis in NAFLD: distinct clinicopathologic meanings. Hepatology. 2011;53:810–20.
29. Joshi-Barve S, Barve SS, Amancherla K, Gobejishvili L, Hill D, Cave M, et al. Palmitic acid induces production of proinflammatory cytokine interleukin-8 from hepatocytes. Hepatology. 2007;46:823–30.
30. Wang X, Zheng Z, Caviglia JM, Corey KE, Herfel TM, Cai B, et al. Hepatocyte TAZ/WWTR1 promotes inflammation and fibrosis in nonalcoholic steatohepatitis. Cell Metab. 2016;24:848–62.
31. Wattacheril J, Issa D, Sanyal A. Nonalcoholic steatohepatitis (NASH) and hepatic fibrosis: emerging therapies. Annu Rev Pharmacol Toxicol. 2018;58:649–62.
32. Lindenmeyer CC, McCullough AJ. The natural history of nonalcoholic fatty liver disease-an evolving view. Clin Liver Dis. 2018;22:11–21.
33. Sutti S, Albano E. Adaptive immunity: an emerging player in the progression of NAFLD. Nat Rev Gastroenterol Hepatol. 2020;17:81–92.
34. Qureshi K, Neuschwander-Tetri BA. The molecular basis for current targets of NASH therapies. Expert Opin Investig Drugs. 2020;29:151–61.
35. Xu WS, Parmigiani RB, Marks PA. Histone deacetylase inhibitors: molecular mechanisms of action. Oncogene. 2007;26:5541–52.
36. Korfei M, Skwarna S, Henneke I, MacKenzie B, Klymenko O, Saito S, et al. Aberrant expression and activity of histone deacetylases in sporadic idiopathic pulmonary fibrosis. Thorax. 2015;70:1022–32.
37. Leoni F, Fossati G, Lewis EC, Lee JK, Porro G, Pagani P, et al. The histone deacetylase inhibitor ITF2357 reduces production of pro-inflammatory cytokines in vitro and systemic inflammation in vivo. Mol Med. 2005;11:1–15.
38. Bettica P, Petrini S, D'Oria V, D'Amico A, Catteruccia M, Pane M, et al. Histological effects of givinostat in boys with Duchenne muscular dystrophy. Neuromuscul Disord. 2016;26:643–9.
39. Singh CK, Nihal M, Ahmad N. Histone deacetylase inhibitory approaches for the management of osteoarthritis. Am J Pathol. 2016;186:2555–8.
40. Louwies T, Ligon CO, Johnson AC, Greenwood-Van Meerveld B. Targeting epigenetic mechanisms for chronic visceral pain: a valid approach for the development of novel therapeutics. Neurogastroenterol Motil. 2019;31:e13500.
41. Wang PX, Ji YX, Zhang XJ, Zhao LP, Yan ZZ, Zhang P, et al. Targeting CASP8 and FADD-like apoptosis regulator ameliorates nonalcoholic steatohepatitis in mice and nonhuman primates. Nat Med. 2017;23:439–49.
42. Li ZZ, Berk M, McIntyre TM, Feldstein AE. Hepatic lipid partitioning and liver damage in nonalcoholic fatty liver disease: role of stearoyl-CoA desaturase. J Biol Chem. 2009;284:5637–44.
43. Sinha RA, Singh BK, Yen PM. Direct effects of thyroid hormones on hepatic lipid metabolism. NatRev Endocrinol. 2018;14:259–69.
44. Chen Z, Yu Y, Cai J, Li H. Emerging molecular targets for treatment of nonalcoholic fatty liver disease. Trends Endocrinol Metab. 2019;30:903–14.
45. Kothari S, Dhami-Shah H, Shah SR. Antidiabetic drugs and statins in nonalcoholic fatty liver disease. J Clin Exp Hepatol. 2019;9:723–30.
46. Adorini L, Pruzanski M, Shapiro D. Farnesoid X receptor targeting to treat non-alcoholic steatohepatitis. Drug Discov Today. 2012;17:988–97.
47. Krenkel O, Puengel T, Govaere O, Abdallah AT, Mossanen JC, Kohlhepp M, et al. Therapeutic inhibition of inflammatory monocyte recruitment reduces steatohepatitis and liver fibrosis. Hepatology. 2018;67:1270–83.

Givinostat attenuates NASH and liver fibrosis
HM Huang et al.

953

48. Loomba R, Lawitz E, Mantry PS, Jayakumar S, Caldwell SH, Arnold H, et al. The ASK1 inhibitor selonsertib in patients with nonalcoholic steatohepatitis: a randomized, phase 2 trial. Hepatology. 2018;67:549–59.

49. Ferrari A, Longo R, Peri C, Coppi L, Caruso D, Mai A, et al. Inhibition of class I HDACs imprints adipogenesis toward oxidative and brown-like phenotype. Biochim Biophys Acta Mol Cell Biol Lipids. 2020;1865:158594.

50. Gaur V, Connor T, Sanigorski A, Martin SD, Bruce CR, Henstridge DC, et al. Disruption of the class IIa HDAC corepressor complex increases energy expenditure and lipid oxidation. Cell Rep. 2016;16:2802–10.

51. Tonini C, Colardo M, Colella B, Di Bartolomeo S, Berardinelli F, Caretti G, et al. Inhibition of bromodomain and extraterminal domain (BET) proteins by JQ1 unravels a novel epigenetic modulation to control lipid homeostasis. Int J Mol Sci. 2020;21:1297.